Soft Matter

Volume 1 | Number 1 | Jan 2013 | Pages 1–100

Soft Matter

www.rsc.org/softmatter

ROYAL SOCIETY
OF CHEMISTRY

www.rsc.org/softmatter

Journal Name

Chemical Conversion of Self-Assembled Hexadecyl Monolayers with Active Oxygen Species Generated by Vacuum Ultraviolet Irradiation in an Atmospheric Environment

Ahmed I. A. Soliman[a], Takashi Ichii[a], Toru Utsunomiya[a], and Hiroyuki Sugimura[a]*

ABSTRACT

Vacuum ultraviolet (VUV, λ = 172 nm) irradiation of alkyl self-assembled monolayers (SAMs) in the presence of dry air alters their surface properties. In this work, UV photochemically prepared hexadecyl (HD)-SAMs on hydrogen-terminated silicon substrates were irradiated by the VUV light in dry air, which generates active oxygen species by excitation of the atmospheric oxygen molecules. These active oxygen species convert the terminal methyl groups of the SAMs to polar functional groups, which were examined quantitatively by X-ray photoelectron spectroscopy (XPS) and chemical labeling. At the first stage of the VUV irradiation, the SAMs' surface was functionalized, and the ratios of the generated polar functional groups markedly increased. With elongation of the irradiation period, the SAMs were gradually degraded, and the total polar group percentages gradually decreased. The difference between the oxygenated carbon components derived by the deconvolution of the XPS carbon (C1s) spectrum and the chemical labeling of polar groups revealed enormous quantities of ethereal and ester groups that cannot react with the labeling agents but are included in the C1s spectral envelope. These modifications were reflected on the SAMs' morphological structures, which were gradually distorted until a complete amorphous structure was obtained after the complete elimination of HD-SAMs.

INTRODUCTION

Alkyl self-assembled monolayers (SAMs) on oxide free silicon (Si) substrates are of great interest for different applications especially electronics, lithography, biomolecule immobilization, and as a anti-stiction coating for microelectromechanical systems (MEMS) due to their chemical durability in the aqueous solution of acids and bases.[1,2] Alkyl-SAMs are considered to be highly stable under different environmental conditions, because the SAMs are attached to the substrates through Si-C covalent bonds.[3–5] The lack of a silicon dioxide (SiO_2) interfacial layer[6,7] enables electron transmission to the substrate via SAMs. Furthermore, alkyl-SAMs were reported to be highly packed and dense on the substrate surface.[4,8] Several methods were reported for alkyl-SAMs preparation on a hydrogen-terminated silicon (H-Si) substrate by heat,[9–11] ultraviolet (UV) exposure,[6,12–14] visible (Vis) light exposure[6,15] and localized surface plasmon.[16]

Recent studies on the photoirradiation of both polymers and SAMs have indicated that irradiation by vacuum ultraviolet (VUV) light of shorter wavelength (172 nm) in the presence of

oxygen is a powerful technique for functionalization of the terminal groups. New polar functional groups such as hydroxy (OH), aldehyde (CHO) and carboxy groups (COOH) were introduced to the terminal groups, and these surface modifications pave the way for advanced applications of microdevices. The introduction of these polar groups is explained on the basis that 172 nm VUV light excites the oxygen molecules resulting in generation of ozone and atomic oxygen in singlet and triplet states.[17,18] These active oxygen species, especially singlet state species, have a strong oxidative power; they oxidize the alkyl-terminated groups (–R) of SAMs and polymers to polar functional groups (OH, COOH and CHO), and convert their surfaces to become more hydrophilic. With elongation of the VUV irradiation period, the backbone of SAMs and polymers is gradually degraded until complete dissociation.[17–19] VUV irradiation of methyl-terminated organosilane SAMs showed that the active oxygen species decayed SAMs' carbon skeleton gradually, by introducing new polar groups, until complete SAMs elimination, and these chemical conversions were reflected on the surface properties, especially wettability. These new polar groups on the SAMs' surface act as anchor groups for multilayer assembly and biomolecule immobilization,[20–23] so that the VUV irradiation offers a significant and accurate method for micro-nanoscale lithography, especially SAMs patterning,[24] and such micro-

[a] Department of Materials Science and Engineering, Kyoto University, Yoshida-hommachi, Sakyo-ku, Kyoto 606-8501, Japan
*E-mail address: sugimura.hiroyuki.7m@kyoto-u.ac.jp

nanopatterned SAMs will be enormously important for different technological applications.[25–27]

Based on quantitative estimation of the chemical constituents using X-ray photoelectron spectroscopy (XPS) peak fitting and derivatization strategies, recent studies have investigated the chemical conversions of polymers and SAMs under different exposure conditions. Trifluoroacetic anhydride (TFAA), 2,2,2-trifluoroethylhydrazine (TFH) and 2,2,2-trifluoroethanol (TFE) are well-known labeling reagents for derivatizing and quantifying the OH, CHO and COOH surface groups of polymers, respectively. These reagents have high reaction selectivity with their corresponding polar groups under non-vigorous reaction conditions.[28–30] After functional group derivatization, a new peak appeared in the XPS C1s spectrum representing CF_3. According to Takabayashi et al., the carbonaceous polymer functional groups on surfaces such as OH, CHO and COOH have different standard reactivities during the reaction with labeling reagents (TFAA, hydrazine, TFE).[31] These labeling reagents are not chemospecific for OH, CHO and COOH.[31–35]

Almost all previous reports have referred to chemical modifications of polymers and SAMs molecules without discerning and realizing the method to achieve these modifications. Realization of polar group formation routes is an extremely difficult and complicated process, but it is a decisive topic for understanding the photochemistry of polymers and SAMs under VUV irradiation. In addition, the chemical and surface properties of alkyl-SAMs that attached to bared silicon through silicon carbon covalent bonds (Si-C) under VUV irradiation have been studied in a few reports without obtaining the photochemical reaction routes and elucidation of their surface property changes.[25] Therefore, we estimated the generated polar groups on alkyl-SAMs qualitatively and quantitatively after different periods of VUV and active oxygen species (VUV/(O)) exposure. We adjusted the derivatization procedures and the calculations to be applicable with SAMs. Furthermore we carefully quantified the chemical constituents of the photomodified SAMs as a factor of the irradiation time, and their influences to the surface and morphological properties. Through the SAMs' chemical constituents and surface properties investigations, we expect to establish the photochemical modification routes and mechanisms, and to explain the origin of the changes in surface properties and morphology under VUV-light exposure.

In this study, the hexadecyl (HD-) SAM was used as alkyl-SAMs, and was prepared by UV light exposure to activate the bonding between H-Si with 1-alkene. Prepared HD-SAM was photomodified under VUV irradiation (λ = 172 nm) for different irradiation periods in dry air. The chemical constituents of photomodified HD-SAM were characterized by XPS and Fourier transform infrared spectroscopy (FTIR)-attenuated total reflectance (ATR), while the polar groups were quantified by XPS C1s peak deconvolution and chemical labeling derivatization. The derivatization reactions of SAMs' polar groups were accomplished by applying TFAA, TFH and TFE reagents. OH, CHO and COOH monofunctional SAMs were used as references for determining the polar groups'

reactivities with the labeling reagents. OH and COOH monofunctional SAMs were formed using 11-mercaptoundecan-1-ol (MUD) and 11-mercaptoundecanoic acid (MUDA) on gold (Au) substrate, respectively, while 11-(triethoxysilyl)undecanal (TESU) was used as the precursor of CHO monofunctional SAM on silicon substrate. Labeling reagents were applied for derivatizing the polar groups of HD-SAMs after different VUV irradiation periods. The modifications of HD-SAMs were reflected in their wettability and their thickness, as determined by water contact angle (WCA) apparatus and ellipsometer, respectively. The morphological changes of SAMs' surfaces were investigated by atomic force microscopy (AFM) alongside the VUV irradiation.

We expected that determining the chemical constituents and the surface property changes of HD-SAM after short irradiation periods would elucidate the different stages and pathways of olefin polymers and alkyl-SAMs oxidation, and clarify the causes of their property changes after different exposure periods.

EXPERIMENTAL METHODS

Hexadecyl Monolayer Formation

HD-SAM was prepared by the hydrosilylation of 1-hexadecene with the H-terminated silicon surface under UV exposure.[6,12–14,36] A phosphorous low-doped n-type silicon (111) wafer with resistivity range from 1- 10 Ω cm was used as a substrate to form the monolayer. The silicon substrates were ultrasonically cleaned in ethanol (Nacalai tesque, 99.5%) and ultrapure water for 20 min, in that order. Further cleaning was conducted for 20 min by VUV light exposure generated from a xenon excimer lamp (Ushio UER 20-172V, UEP20, wavelength (λ) = 172 nm, and power density = 10 mW cm^{-2}) to remove the organic impurities. H-terminated silicon substrates were obtained by treating the cleaned substrates with HF (Stella Chemif, 5%) for 5 min at room temperature, followed by immersion in 40% NH_4F (Daikin) for 30 sec at 80 °C. the formation of HD-SAMs was accomplished by transferring the H-terminated silicon substrate to a photocell containing 1-hexadecene (Tokyo chemical industry (TCI), 99 %) as a monolayer precursor under a continuous N_2 flow, followed by UV light exposure. The UV-light generated from a high-pressure mercury lamp (Ushio USH-500D) was focused on the silicon surface, and the light intensity at the substrate surface was 500 mW cm^{-2}. The UV-light exposure was continued for one hour, then the fabricated silicon substrates were ultrasonically cleaned in n-hexane (Nacalai Tesque, 96 %), ethanol and ultrapure water for 10 min, in that order, to remove any excess physisorbed precursor.

VUV modification of HD-SAMs

The VUV irradiation of HD-SAMs was performed using another xenon excimer lamp with the same specifications. The irradiation was done at atmospheric pressure under a flow of dry air, and the distance between HD-SAM and the lamp window was maintained at 30 mm as illustrated in Fig. 1. The

transmittance of 172 nm VUV through the 30 mm air layer was estimated to be nearly 0.1 %, so that the SAMs modifications were only attributed to the influence of active oxygen species. The properties of the VUV modified-SAMs were examined for 3000 sec of irradiation time by obtaining their WCA values, thickness, chemical constituents and morphological changes.
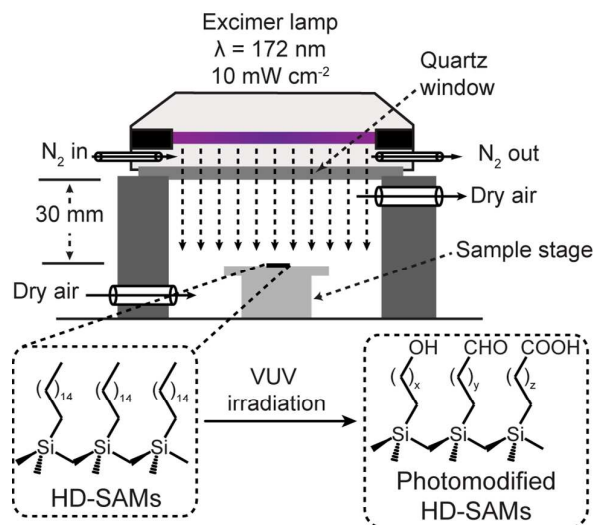

Fig. 1. Schematic illustration of VUV irradiation apparatus of HD-SAMs.

Chemical labeling of the generated polar functional groups

Labeling of the oxygenated groups was conducted using TFAA (TCI, 98%, *corrosive on skin contact and danger on inhalation*), TFH (Sigma Aldrich, 70 % aqueous solution) and TFE (TCI, 99%) reagents, which derivatized the OH, C=O and COOH groups, respectively. The as-prepared HD-SAM and photomodified HD-SAMs were derivatized in 1 mL of TFAA acidified by 0.01 mL of H_2SO_4 (TCI, 98 %) for 3.0 h at room temperature. The immersion period of SAMs in acidified TFH was 5.0 h, and 2.5 h in acidified TFE. The derivatized HD-SAMs were rinsed in ethanol and ultrapure water for cleaning. Then SAMs were transferred to the XPS chamber to investigate their chemical constituents. The reactivates of the labeling reagents with the corresponding functional groups are significantly important for the accurate estimation of the functional groups' percentages. The OH and COOH-terminated SAMs on gold (Au) were used for determining the reaction reactivities between the terminal moieties (OH and COOH) and the labeling reagents. Each gold substrate (100 nm thick gold film) was prepared on a silicon plate covered by a titanium (Ti) adhesion layer (10 nm in thickness) by vacuum evaporation.

The OH-terminated SAM was prepared by immersing the gold substrate in 0.1 mM of MUD (Sigma Aldrich, 97 %) ethanolic solution at 80 °C for 15 min. The prepared SAM was rinsed with ethanol and ultrapure water for cleaning, while the COOH-terminated SAM was prepared using MUDA (Sigma Aldrich, 95%) with the same procedures as for the OH-terminated SAM on the gold substrate. The CHO-terminated SAM on silicon substrates was prepared by the chemical vapor deposition (CVD) process,[37] A silicon substrate was cleaned

and transferred to a Teflon container (120 cm^3). A small glass cup filled with 30 µL of TESU (Gelest, 95%) was also transferred to the Teflon container, then the container was sealed well and heated at 135 °C for 2 hours. The sample substrate was cleaned ultrasonically in ethanol for 5 min followed by sonication in ultrapure water at 5 min as well. These reference SAMs were derivatized in the same manner as for labeling of HD-SAM.

Analytical methods

The as-prepared and photomodified HD-SAMs were examined through the determination of WCA, thickness, chemical constituents and surface morphology. The WCA values of as-prepared and photomodified SAMs were measured with a static contact angle meter (Kyowa Interface Science CA-X Co., DM 500). The water droplet volume was fixed at 1.8 µL. The thicknesses of the fabricated SAMs were measured by a spectroscopic ellipsometer (Otsuka Electronics FE-5000). The air/organic film/Si model was used for obtaining the thicknesses of the samples. The incident angle was set at 70°, and the measured wavelength range was 400 nm to 800 nm. The refractive index of SiO_2 was adopted as that of the monolayer film over the measured wavelength range, where the SiO_2 and the monolayer were transparent.[6,37] Both thickness and WCA measurements were carried out three times for every sample. XPS was used for qualitative and quantitative examination of the chemical constituents of SAMs using the ESCA-3400 system (Kratos Analytical) with a Mg Kα X-ray source operated at 10 kV and 10 mA. The background of pressure for analysis was less than 5×10^{-6} Pa, The XPS' obtained spectra were referenced to Si-Si peak at 99.6 eV.[6,38] FT-IR (Diglab Japan Co., Excalibur FTS-3000) was used for investigating the functional groups formed on the modified-SAMs. The attenuated total reflection (ATR) configuration was used with a germanium (Ge) crystal. The spectral resolution was 4 cm^{-1}, and a 1024 scan cycle was used. AFM (MFP-3D, Oxford Instruments) was used to examine the surface morphology of the as-prepared HD-SAM and the VUV influence on the surface morphology of the modified-SAMs. AC mode was used to obtain topographic images of samples by employing aluminum backside coated Si probes (SII Nanotechnology Inc., SI-DF-20).

RESULTS AND DISCUSSION

Changes in WCA and thickness of SAMs

Fig. 2 shows that the values of SAMs' WCA and thicknesses decreased with increasing irradiation time up to 3000 sec. Based on WCA and thickness decrease rates, SAMs' WCA and thicknesses were changed in three stages labeled [i], [ii] and [iii]. Fig. 2 (A) shows that SAMs' WCA at the initial 260 sec of VUV irradiation (stage [i]) decreased from 105.6° (± 0.9) to 78.9° (± 0.7), while at stage [ii] (from 260 sec to 1800 sec of VUV irradiation), the WCA values decreased from 68.3° (± 0.3) to 5° (± 0.4). After elongation of the irradiation time to 1800 sec or more (stage [iii]), dropped water was diffused on the

substrate surface and the WCA value became nearly 0°. The decrease in the WCA values is attributed to the surface hydrophilicity increase, namely, an increase in hydrophilic groups generated on surface such as OH, CHO and COOH groups, in addition to the decrease of hydrophobicity by shortening the hydrophobic backbone length of each SAM.[17–23,25,26]

Shortening of the hydrophobic backbone was confirmed by measuring the SAMs' thickness values as shown in Fig. 2 (B). These obtained thicknesses are not absolutely accurate, due to the uncertainty of the refractive indices of the modified SAMs. However, these values are considered to be sufficiently accurate for the relative comparison in the thickness of SAM. The results clearly indicate the decay of SAMs' thickness with increasing the VUV/(O) irradiation time. At stage [i], the thickness shows a greater decrease rate - from 2.65 nm to 2.46 nm - than the decrease rate in stage [ii]. At stage [ii], the thickness decreased from 2.39 nm to 1.81 nm. After reaching stage [iii], the thickness was nearly constant between 1.81 nm ~ 1.85 nm. The generation of surface polar groups and thickness decrease could be explained by the active oxygen species approaching and oxidizing the terminal alkyl groups of SAMs with the introduction of new polar groups. With further species exposure the new polar groups were degraded and new groups formed, so addition and dissociation of polar groups were successive and correlated processes. At the first stage ([i]), the introduction of polar groups on the SAM surface (functionalization process) was considered the main process, while the degradation process was dominant during the second stage ([ii]). At the final stage ([iii]), SAMs were completely degraded and removed, while the substrate silicon surface was converted to SiO_2.
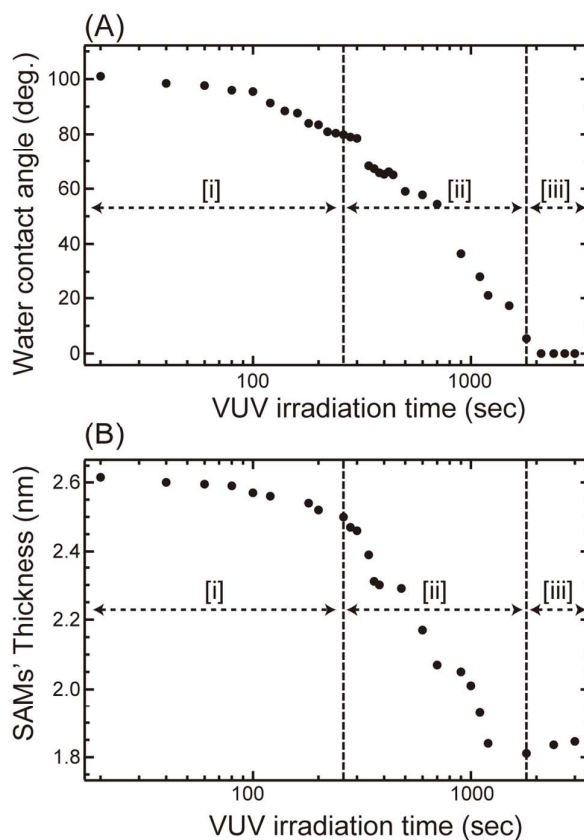

Fig. 2. Changes in (A) WCA and (B) thickness of HD-SAMs with irradiation time of VUV light.

The chemical changes of SAMs

For the surface chemical analysis of the modified SAMs, we employed ATR-FTIR and XPS measurements. The ATR-FTIR spectrum of HD-SAM (Fig. 3) shows bands at 1334 cm^{-1}~1446 cm^{-1}, 2857 cm^{-1}, 2925 cm^{-1} and 2959 cm^{-1}, which represent C-H bending bands (rocking and scissoring), $-CH_2-$ stretching symmetric (v_s), $-CH_2-$ asymmetric (v_{as}) and C-H stretching asymmetric of CH_3 (v_{as}), respectively. Si-OH and Si-O-Si bands also appeared at 846 cm^{-1} and 1109 cm^{-1}, respectively. After the VUV/(O) irradiation, new functional groups were observed as shown after 250 sec, 500 sec and 1000 sec of VUV irradiation. These new bands appeared at 1221 cm^{-1}, 1716 cm^{-1} and 3454 cm^{-1}, which corresponded to C-O (str), C=O (str) and OH (str), respectively.[22] At 1643 cm^{-1}, the absorbance band indicates that hydrogen bonding occurred between COOH and OH groups.[39,40] According to the new bands observed, the modified-SAMs' surface became more hydrophilic with increased presence of polar groups (O-H, C=O and COOH groups).
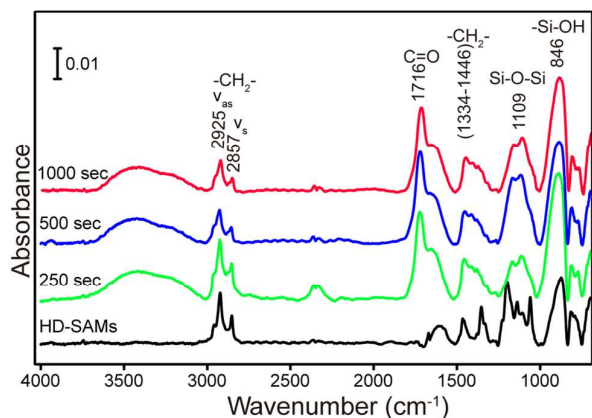
Fig. 3. ATR-FTIR spectra of the HD-SAMs surfaces before and after VUV irradiation for 250, 500 and 1000 sec.

XPS investigations of SAMs irradiated for different irradiation periods indicated that the chemistry of SAMs changed dramatically as illustrated by the XPS spectra (Fig. 4). The atomic percentage of carbon decreased, but the oxygen percentage increased with the irradiation time as shown in Fig. 4 (A) and (B), respectively. The increase of oxygen is ascribed to both the polar groups formation "photofunctionalization" and the growth of the SiO_2 layer as mentioned in Fig. 4 (C). In contrast, the XPS C1s peak deconvolution before irradiation indicated only one peak at 285.0 eV, which belongs to C-C backbone of HD-SAM. After irradiation, new oxygenated groups C-O, C=O and COO were found at binding energies of 286.8 eV, 288.0 eV and 289.0 eV, respectively. The decrease of carbon percentage was reflected in the decrease of hydrophobic chain thickness, while the polar group presence indicates that SAMs terminal groups were converted to hydrophilic groups. With increasing VUV exposure time, the SiO_2 layer thickness increased as shown in the XPS Si2p peak (Fig. 4 (C)). The Si2p XPS peak shows two peaks at 99.5 eV and 103.6 eV, which were belonged to Si-Si and SiO_2, respectively.
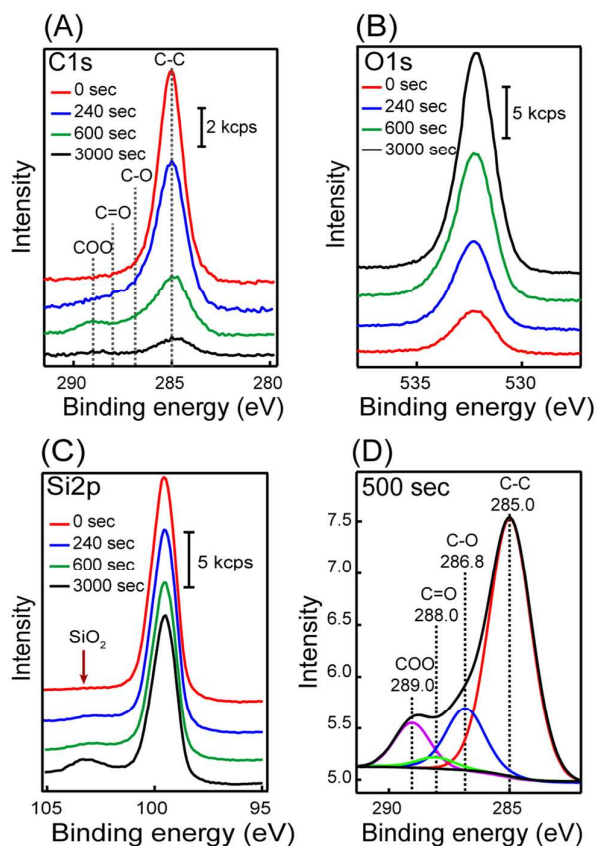

Fig. 4. XPS (A) C1s, (B) O s, and (C) Si2p spectra of the HD-SAMs surfaces before and after VUV light irradiation. (D) Deconvoluted XPS C1s spectrum of the HD-SAM at 500 sec of VUV light irradiation.

The spectrum of XPS C1s was deconvolved for qualitative and quantitative estimation of the oxygenated groups attached to carbon as shown in Fig. 4 (D), which illustrates the C1s spectrum fitting for the 500-sec VUV-modified-SAMs. The qualitative analysis was achieved by spectrum deconvolution of C1s and obtaining the values of binding energies of each deconvoluted peaks. The binding energies were 285.0 eV, 286.8 eV, 288.0 eV and 289.0 eV for C-C, C-O, C=O and COO, respectively. The quantitative analysis was performed by fixing the full width at half maximum (FWHM) of these peaks at 1.80 eV, 1.82 eV, 1.87 eV and 2.10 eV for C-C, C-O, C=O and COO peaks, respectively. By evaluating the areas under peaks and total atomic percentages of carbon, the polar groups' percentages were calculated using equations (1), (2), (3) and (4) (Chart 1), and the calculated percentages were related to the SAMs' total chemical constituents; P_{C-C}, P_{C-O}, $P_{C=O}$ and P_{COO} represent the percentages of C-C, C-O, C=O and COO functional groups, respectively, while A_{C1s}, A_{C-C}, A_{C-O}, $A_{C=O}$ and A_{COO} represent the area under peaks of C1s, C-C, C-O, C=O and COO, respectively as shown in Fig. 4 (D).

$$P_{C-C} = \frac{A_{C-C} \times \text{atomic\% of C1s}}{A_{C1s}} \quad (1)$$

$$P_{C-O} = \frac{A_{C-O} \times \text{atomic\% of C1s}}{A_{C1s}} \quad (2)$$

$$P_{C=O} = \frac{A_{C=O} \times \text{atomic\% of C1s}}{A_{C1s}} \quad (3)$$

$$P_{COO} = \frac{A_{COO} \times \text{atomic\% of C1s}}{A_{C1s}} \quad (4)$$

Chart 1. Equations 1, 2, 3 and 4 used to calculate the atomic percentages of C-C, C-O, C=O and COO components of HD-SAMs.
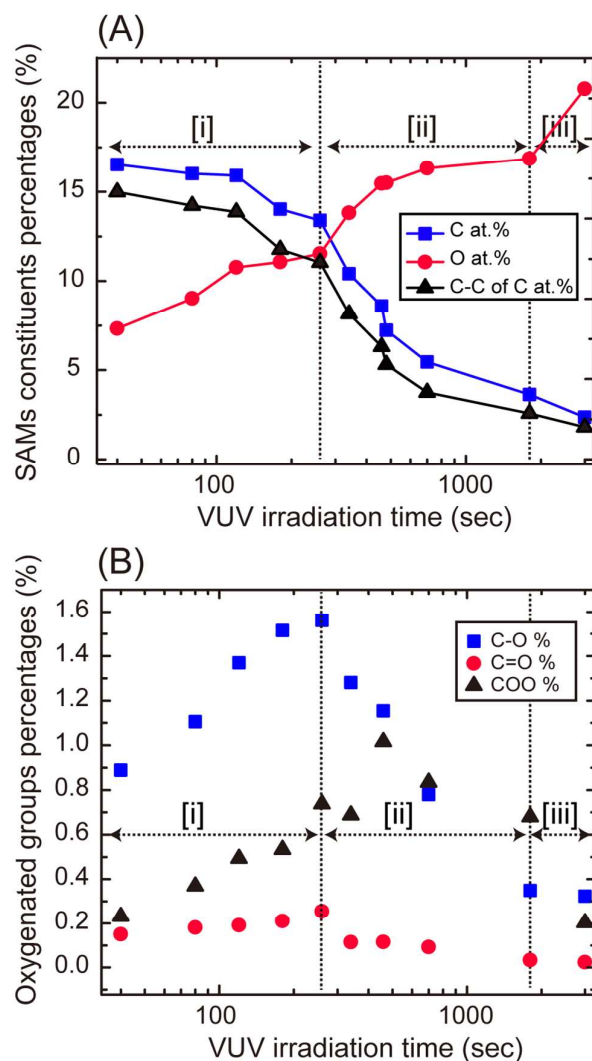

Fig. 5. Chemical constituents changes of HD-SAMs with VUV irradiation. (A) The atomic percentage changes of HD-SAMs' chemical constituents with VUV irradiation time. (B) The changes of polar groups' percentages with VUV irradiation time.

Fig. 5 (A) shows the atomic percentages of oxygen, carbon and carbon representing C-C of HD-SAMs changes with VUV irradiation time; the atomic percentage of oxygen increased with increasing irradiation time, while the atomic percentage of carbon decreased. The decrease rate of carbon percentage in stage [i] was slower than at stage [ii], which indicates that the carbon dissociation at stage [ii] was higher than at stage [i]. The increase rate of oxygen percentage was higher in stage [i] than in stage [ii], reflecting the increase of the percentages of polar groups on SAMs. At stage [iii], carbon's percentage was very small, and the SAMs were completely removed. The carbon skeleton of HD-SAM was gradually dissociated in the same manner of total carbon decrease as seen from the atomic percentages of C-C. The difference between the percentages of carbon and C-C represents the percentages of generated polar groups on the surface of SAMs. Fig. 5 (B) shows the changes of polar groups' percentages of SAMs with VUV irradiation time. This figure explains the origin of these modifications in the stages [i], [ii] and [iii], which were distinguished and matched with those obtained from WCA and thickness changes. At stage [i], the polar groups increased; the percentage of C-O increased from 0 % to 1.56 %, while C=O increased from 0 to 0.35%. But at stage [ii], both C-O and C=O groups' percentages decreased to 0.35 % and 0.02 %, respectively, while the increasing of COO groups continued until 460 sec. The relatively low percentages of C=O groups were attributed to the rapid oxidation of C=O to COO groups. The COO groups' percentage increased rapidly during the first 460 sec of VUV irradiation from 0 % to 1.02 %. After 460 sec, the COO groups' percentage decreased to 0.68. The continuity of COO groups' percentage increasing until 460 sec signified that the formation of COO groups was produced from the oxidation of C-O and C=O groups. The polar groups' percentages at stage [i] were high, which explains the rapid decrease of WCA. The SAMs terminal groups were oxidized through adding oxygen to form OH groups, and these OH groups were then converted directly to CHO groups, which converted rapidly to COOH groups. Other groups such as ethereal, ketone and ester groups could be formed through condensation reactions between the surface groups. Further light exposure degraded the terminal groups of the SAMs until complete degradation of SAMs as illustrated in Scheme 1.
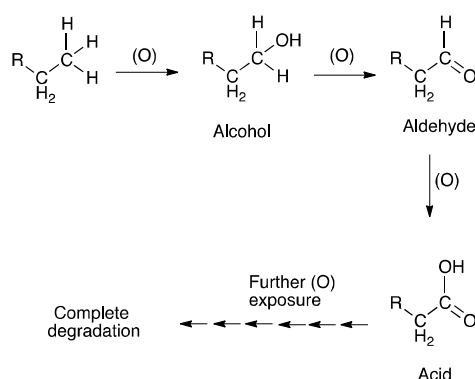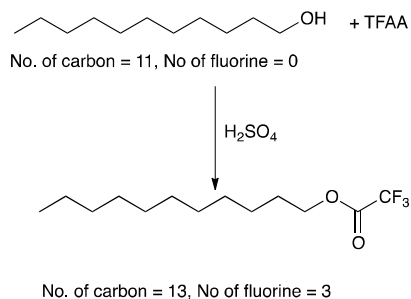

Scheme 1. Illustration of the routes of functionalization and degradation of alkyl-SAMs under streams of VUV/(O).

COMMUNICATION

Chemical labeling of polar functional groups

In principle, XPS can be used to determine the local bonding environments of carbon atoms such as C-O, C=O and COO groups based on the chemical shift in the binding energy. However, spectral deconvolution of the XPS C1s spectra is not suitable for identifying the functional groups at the same component of an XPS peak, such as OH and ethereal (C-O-C) functional groups. Therefore, we performed chemical labeling reactions to identify the OH, CHO and COOH terminal polar groups from ethereal (C-O-C), ketone (C-CO-C) and ester (C-COO-C) terminal groups. The ethereal and ester groups could not react with the derivatization reagents and situated inside the XPS C1s envelope, so that the ethereal and ester groups were quantified as the difference between total estimated groups from XPS C1s peak deconvolution and calculated from labeling reactions. The percentage of C-O detected from C1s XPS peak deconvolution contains both OH and ethereal groups. Only OH groups were detected from the labeling reaction. Ethereal groups were quantified as the difference between the results of XPS peaks deconvolution and labeling. Table 1 presents the reaction reactivities of functional groups with the labeling reagents. These reactivities were calculated from the percentages of fluorine and carbon detected by XPS as shown in Chart 2 (equations (5), (6) and (7)). For clarification, if the reaction between 1-undecanol and TFAA was accomplished to 100 %, three fluorine atoms and two carbon atoms would be added to it, and the carbon atoms would be increased to 13. The theoretically-calculated ratio of F/C equals 3/13. Practically, the F/C ratio detected by XPS did not achieve this theoretical ratio, so the reaction reactivity of reagent with polar group ($R_{reagent/functional\ group}$) is equal to the practical ratio of F/C to the theoretically-calculated ratio of F/C. $R_{TFAA/OH}$, $R_{TFH/CHO}$ and $R_{TFE/COOH}$ were 66.2%, 92.2% and 59.7%, respectively. The lower reaction reactivities of OH and COOH groups with the labeling reagents are attributed to steric hindrance, rapid reversible reaction, hydrogen bonding between the functional groups, and their actual reactivity with the reagents,[39,41] while CHO cannot form hydrogen bonds, and its condensation reaction with TFH is almost irreversible.[42]

Chart 2. Illustration of OH group labeling calculation of 1-undecanol with TFAA via equations 5, 6 and 7 to calculate the reagents' reactivity with polar groups.

$$\text{Theoretical ratio of } \frac{F1s}{C1s}(100\% \text{ accomplished reaction}) = \frac{3}{13} \quad (5)$$
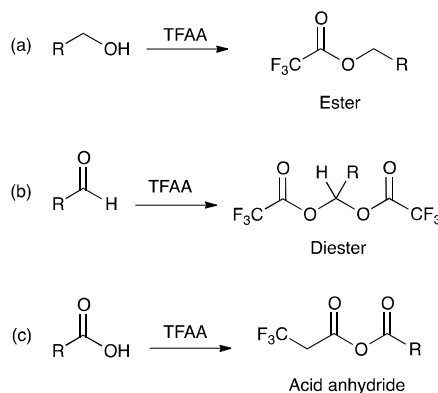
$$\text{Practical ratio of } \frac{F1s}{C1s}(\text{estimated from XPS}) = \frac{\text{Atomic\% of F1s}}{\text{Atomic\% of C1s}} \quad (6)$$

$$R_{reagent/functional\,groups} = \frac{(F/C)_{practically}}{(F/C)_{Theoretically}} \quad (7)$$

A new peak representing CF_3 appeared in the XPS C1s spectrum of the labeled HD-SAMs at 293.46 eV, 293.12 eV and 293.38 eV after TFAA, TFH and TFE labeling as shown in Fig. 6 (A'), (B') and (C'), respectively. Fig. 6 (A), (B) and (C) show the XPS F1s spectra detected after TFAA, TFH and TFE derivatization at binding energies 690.24 eV, 689.53 eV and 689.81 eV, respectively. The binding energy variations of both F1s and CF_3 peaks were attributed to the different environmental composition of adjacent groups attached to CF_3 as shown in Schemes 2, 3 and 4.

Fig. 6 (A), (B) and (C) show the increase of fluorine percentages after TFAA, TFH and TFE labeling at the beginning of VUV exposure, and decreased after longer irradiation periods. Variation of the fluorine's percentages explains the variation of the percentages of polar groups on the surface with irradiation time. Using Chart 3 (equations (8) and (9)), the percentages of OH, CHO and COOH groups were quantitatively estimated for the three stages.

Table 1. Reaction reactivities of functional groups with TFAA, TFH, TFE labeling reagents.

Functional groups	Reaction reactivities		
	R_{TFAA}	R_{TFH}	R_{TFE}
CHO	29.4 (± 3.8)	92.2 (± 5.6)	37.9 (± 4.7)
COOH	16.7 (± 1.0)	40.2 (± 4.9)	59.7 (± 1.9)
OH	66.2 (± 1.0)	30.2 (± 2.9)	15.6 (± 1.9)

Scheme 2. Schematic illustration of the reaction between TFAA reagent with OH, CHO, COOH groups.

COMMUNICATION   Journal Name

Soft Matter Accepted Manuscript
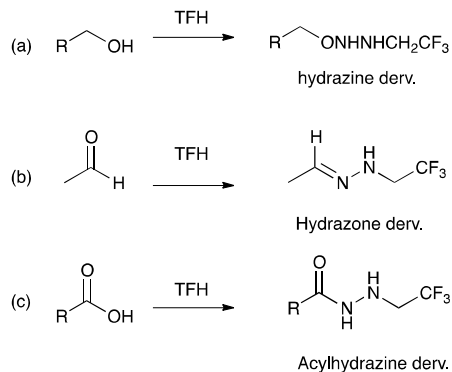
Scheme 3. Schematic illustration of the reaction between TFH reagent with OH, CHO, COOH groups.
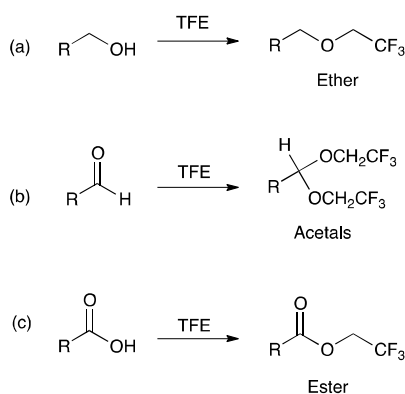
Scheme 4. Schematic illustration of the reaction between TFE reagent with OH, CHO, COOH groups.
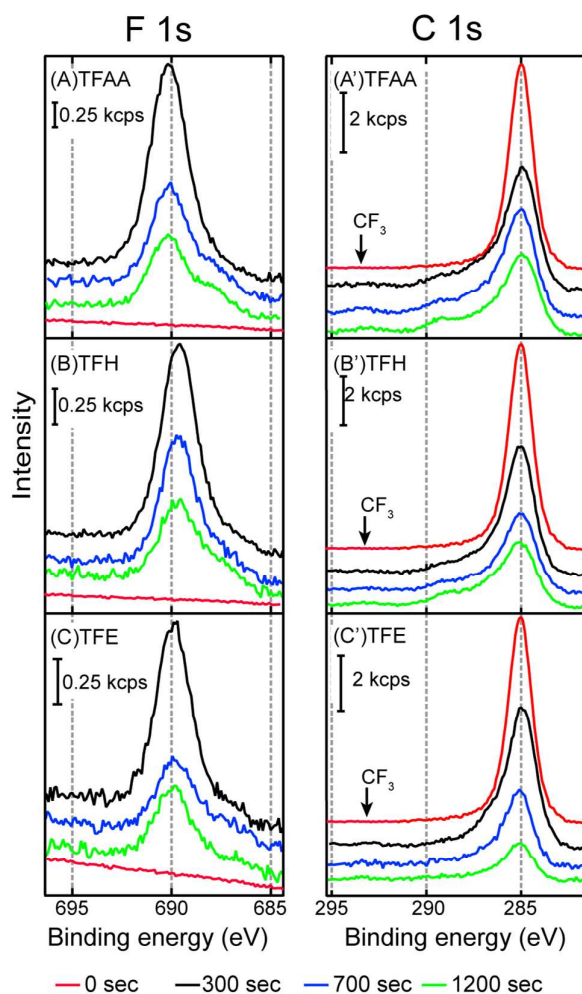

Fig. 6. XPS F1s spectra of (A) TFAA, (B) TFH and (C) TFE labeled VUV irradiated HD-SAMs. (A'), (B') and (C') represent C1s spectra of TFAA, TFH and TFE labeled HD-SAMs at different irradiation times.

The percentages of the polar groups were calculated using equations (8) and (9), where F_{TFAA}, F_{TFH} and F_{TFE} represent the fluorine percentages detected after labeling using TFAA, TFH and TFE, respectively, while P_{OH}, P_{CHO} and P_{COOH} represent the detected percentages of OH, CHO and COOH, respectively. $R_{reagent/functional\ group}$ represents the reaction reactivity of the labeling reagent with functional groups as shown in table 1, multiplication by 1/3 is due to 3 fluorine atoms as mentioned from one polar groups derivatization.

$$\frac{1}{3}\begin{bmatrix} F_{TFAA} \\ F_{TFH} \\ F_{TFE} \end{bmatrix} = \begin{bmatrix} R_{TFAA/OH} & R_{TFAA/CHO} & R_{TFAA/COOH} \\ R_{TFH/OH} & R_{TFH/CHO} & R_{TFH/COOH} \\ R_{TFE/OH} & R_{TFE/CHO} & R_{TFE/COOH} \end{bmatrix} \times \begin{bmatrix} P_{OH} \\ P_{CHO} \\ P_{COOH} \end{bmatrix} \quad (8)$$

$$\begin{bmatrix} P_{OH} \\ P_{CHO} \\ P_{COOH} \end{bmatrix} = \frac{1}{3}\begin{bmatrix} R_{TFAA/OH} & R_{TFAA/CHO} & R_{TFAA/COOH} \\ R_{TFH/OH} & R_{TFH/CHO} & R_{TFH/COOH} \\ R_{TFE/OH} & R_{TFE/CHO} & R_{TFE/COOH} \end{bmatrix}^{-1} \times \begin{bmatrix} F_{TFAA} \\ F_{TFH} \\ F_{TFE} \end{bmatrix} (9)$$

Chart 3. Equations 8 and (9) used to calculate the percentages of labeled polar groups.
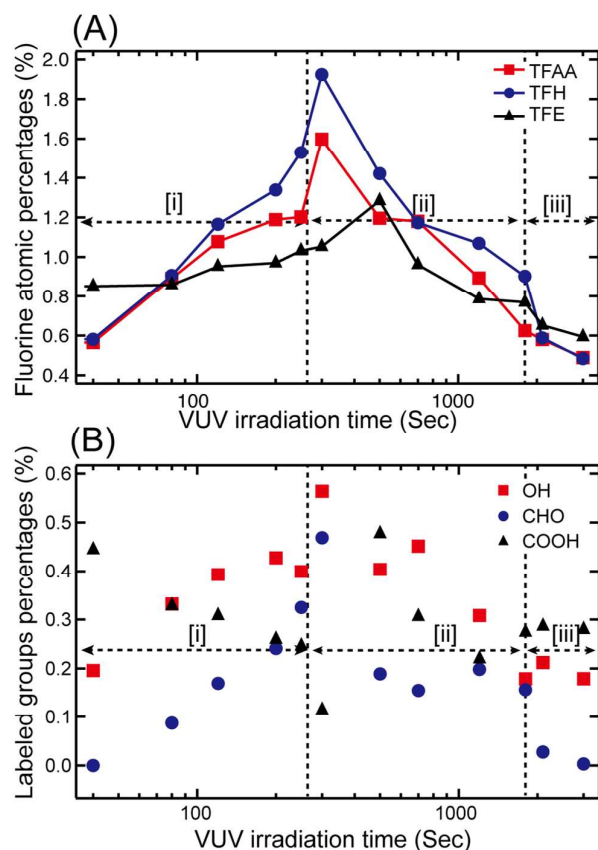
Fig. 7. (A) Atomic percentages of fluorine determined by XPS versus VUV-light treatment time. (B) Calculated oxygenated groups percentages from equations (8) and (9) at different VUV irradiation time.

According to Fig. 7 (A), the detected percentages of fluorine in the photomodified-SAMs increased after derivatization in the first stage and then decreased in the second stage [ii]. These fluorine percentages were used in calculating the polar groups on the surface as shown in equations (8) and (9). Fig. 7 (B) shows a schematic representation of polar groups' percentages calculated using equations (8) and (9) at different VUV irradiation periods. The percentages of OH groups calculated using F1s % in HD-SAM were less than 35 % of the total C-O calculated from XPS C1s peak deconvolution. The percentages of CHO groups detected by XPS and labeling at stage [i] show the relative compatibility, which indicate that the labeling reactivity of ketone ($R_2C=O$) was close to that of aldehyde (RCHO). At stage [ii], however, the detected percentages of CHO groups by labeling were higher than the percentages detected by peak deconvolution, but that is not plausible, and the error is attributed to an XPS analysis limitation due to the small amounts of CHO. The percentages of COO groups detected by TFE labeling were less than that detected by the XPS C1s peak deconvolution. During the stage [i], COOH groups decreased, because the amounts of COOH formed were rapidly decomposed. While at stage [ii], the determined percentages of COOH were higher than at stage [i], because the surface was completely functionalized

and large amounts of OH and CHO groups were converted to COOH groups. In general, the difference between labeling results and XPS C1S peak deconvolution results could be explained by the presence of ethereal and ester groups, which could not be labeled, the presence of polar groups in bulk (enveloped groups), and the limitation of XPS peak deconvolution.

Morphological examination of the surface

Fig. 8 (A) shows an AFM image of the naked H-Si substrate. The image illustrates the terraces separated by monoatomic steps of approximately 0.3 nm height, which is consistent with the monoatomic steps of Si (111) plane. The AFM topography of the HD-SAM is shown in Fig. 8 (B). The stairlike structure of the terraces and monoatomic steps is similar to that of the H-Si surface, which indicates that the HD-SAM is highly arranged.[43] At 250 sec of VUV/(O) irradiation, the substrate's terraces were clearly observed, and no distortions were seen as shown in Fig. 8 (C). This stability and uniformity of the substrate surface indicates that the HD-SAM protected the substrate surface from oxidation. Only the outermost surfaces of the SAMs were modified, and the backbone of the SAMs was gradually dissociated homogenously at all points of SAMs' surface. The VUV/(O) did not dissociate the Si-C bond directly without gradual dissociation of the SAMs' carbon skeleton. After 500 sec, the atomic steps and terraces were still clearly visible with slight distortions as shown in Fig. 8 (D). Under the streams of VUV/(O), the H-Si substrate surface was oxidized to SiO_2 amorphous layers,[20,22] which agreed well with the XPS results (Fig. 4(C)). After 3000 sec of VUV light irradiation, HD-SAM was completely removed and amorphous surface was obtained as shown in Fig. 8 (E).
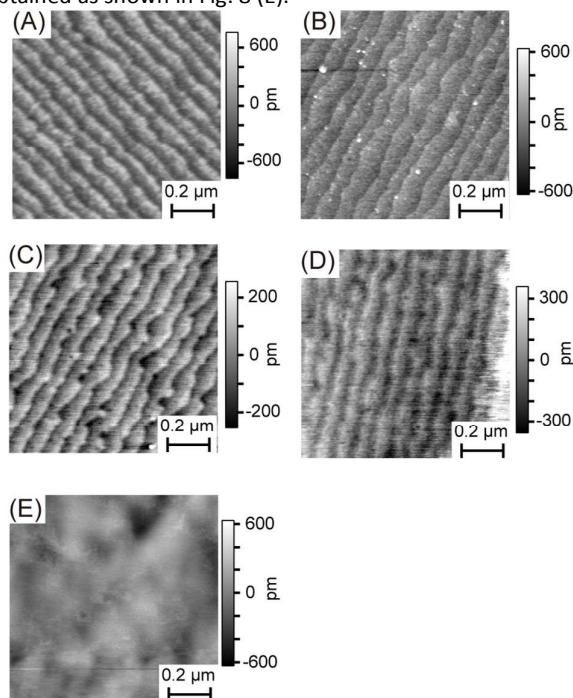
Fig. 8. (A) and (B) are topographic images of H-Si substrate and HD-SAM, respectively. While (C), (D) and (E) are the topographic images of photomodified HD-SAMs after 250 sec, 500 sec and 3000 sec of VUV irradiation, respectively.

The chemistry of photomodified HD-SAMs and their labeling deficiencies are explained in Scheme 5, which is based on the surface properties and chemical constituents of SAM. At stage [i], the SAMs surface was functionalized with different polar groups. With increasing irradiation (stage [ii]), SAMs were rapidly and continuously degraded. After the HD-SAM degradation, the surface was covered with SiO_2 and some carbonaceous impurities.[20] Deficiencies of oxygenated groups labeling were attributed to the presence of ester and ethereal groups, in addition to groups sunken inside SAMs (enveloped groups). Based on all the results, SAMs modifications proceeded in two consequent and correlated processes. At first, the functionalization process occurred at higher rate than the degradation process and was the predominant process, where alkyl terminated groups were oxidized to hydroxyl groups followed by conversion of OH to CHO, while the COOH groups formation were considered the last oxidation process step. With prolonged irradiation period, the SAMs backbone degraded rapidly with accompanying functionalization of terminal groups until complete SAM degradation.
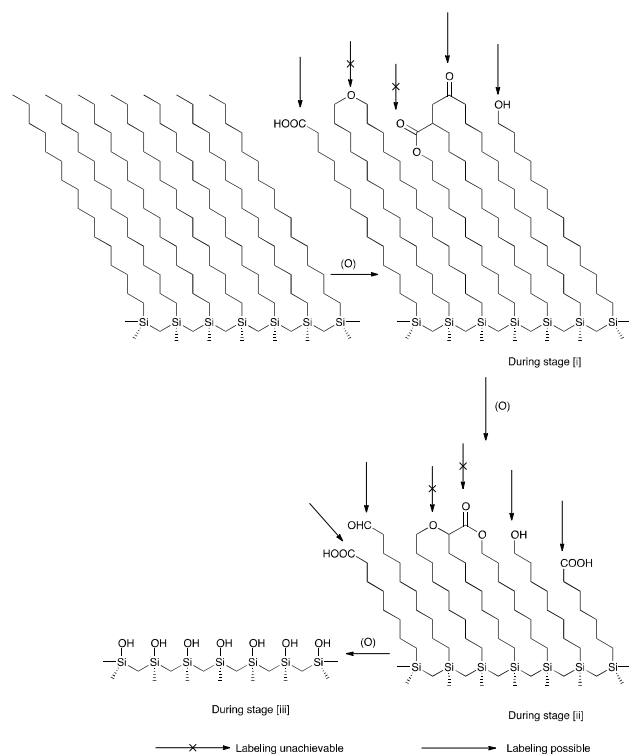
Scheme 5. Schematic illustration of SAMs chemistry during different VUV/(O) irradiation stages and the labeling deficiencies of the new polar groups.

Conclusions

Modification of HD-SAM using the active oxygen species generated by VUV irradiation changed its surface physical and chemical properties. These changes were accomplished in three stages, the division of these stages being based on the different decrease rates of WCA and thickness, in addition to the chemical constituent and morphological changes. These active oxygen species, generated from atmospheric air by the VUV light excitation, oxidized the methyl-terminated groups, and introduced new polar groups. The SAMs' modifications were attributed to the influence of the active oxygen species only. The influence of VUV was almost cancelled by fixing the distance between SAMs and the VUV light source at 30 mm, the VUV light intensity at the SAMs surface was nearly 0.1%. The modifications were accomplished through the photofunctionalization and photodegradation processes. At the first stage, SAMs WCA and thickness decreased, while the polar groups' percentages increased. Labeling of the polar groups reflected the presence of ethereal and ester groups in addition to OH, C=O, CHO and COOH groups. In this stage photofunctionalization was the predominant process, and the SAMs' morphology was preserved without distortion.

At the second stage, photodegradation of the oxygenated groups was the prevailing process. The thickness, WCA and polar groups' percentages of modified-SAMs decreased at different rates than during the first stage. Morphological distortions appeared and increased with irradiation time increase.

At the third stage, the HD-SAM was removed completely from the substrate' surface, and the morphology of H-terminated silicon was completely distorted. The amorphous surface was investigated, and the values of WCA reached 0° without any changes in the obtained thickness.

Combining the XPS measurements with the chemical labeling enhanced our understanding of the chemistry of the VUV modified-SAMs, especially the composition of the terminal functional groups. These investigations help to clarify the photochemical reaction mechanism of the alkyl-SAMs and olefin polymers induced by the VUV light irradiation.

Acknowledgements

Notes and references

1. J. M. Buriak, *Chem. Rev.*, 2002, **102**, 1271–1308.
2. H. Sugimura, in *Nanocrystalline Materials*, Elsevier, London, UK, second., 2012, pp. 161–193.
3. H. Sano, H. Maeda, T. Ichii, K. Murase, K. Noda, K. Matsushige and H. Sugimura, *Langmuir*, 2009, **25**, 5516–5525.
4. H. Sugimura, H. Sano, K. H. Lee and K. Murase, *Jpn. J. Appl. Phys.*, 2006, 45, 5456–5460.
5. M. M. Sung, G. J. Kluth, O. W. Yauw and R. Maboudian, *Langmuir*, 1997, **13**, 6164–6168.

COMMUNICATION

6. H. Sano, H. Maeda, S. Matsuoka, K.-H. Lee, K. Murase and H. Sugimura, *Jpn. J. Appl. Phys.*, 2008, **47**, 5659–5664.

7. W. R. Ashurst, C. Yau, C. Carraro, C. Lee, G. J. Kluth, R. T. Howe and R. Maboudian, *Sensors Actuators A*, 2001, **91**, 239–248.

8. M. R. Kosuri, H. Gerung, Q. Li, S. M. Han, P. E. Herrera-Morales and J. F. Weaver, *Surf. Sci.*, 2005, **596**, 21–38.

9. A. B. Sieval, V. Vleeming, H. Zuilhof and E. J. R. Sudhölter, *Langmuir*, 1999, **15**, 8288–8291.

10. M. Nakano, T. Ishida, H. Sano, H. Sugimura, K. Miyake, Y. Ando and S. Sasaki, *Appl. Surf. Sci.*, 2008, **255**, 3040–3045.

11. M. R. Linford and C. E. D. Chidsey, *J. Am. Chem. Soc.*, 1993, **115**, 12631–12632.

12. F. Effenberger, G. Götz, B. Bidlingmaier and M. Wezstein, *Angew. Chem. Int. Ed.*, 1998, **37**, 2462–2464.

13. M. P. Stewart and J. M. Buriak, *J. Am. Chem. Soc.*, 2001, **123**, 7821–7830.

14. H. Sano, K. Ohno, T. Ichii, K. Murase and H. Sugimura, *Jpn. J. Appl. Phys.*, 2010, **49**, 01AE09 (1–5).

15. M. U. Herrera, T. Ichii, K. Murase and H. Sugimura, *J. Colloid Interface Sci.*, 2013, **411**, 145–51.

16. H. Sugimura, S. Mo, K. Yamashiro, T. Ichii and K. Murase, *J. Phys. Chem. C*, 2013, **117**, 2480–2485.

17. H. Sugimura, K.-H. Lee, H. Sano and R. Toyokawa, *Colloids Surfaces A*, 2006, **284-285**, 561–566.

18. H. Sugimura, L. Hong and K.-H. Lee, *Jpn. J. Appl. Phys.*, 2005, **44**, 5185–5187.

19. C. Elsner, S. Naumov, J. Zajadacz and M. R. Buchmeiser, *Thin Solid Films*, 2009, **517**, 6772–6776.

20. Y.-J. Kim, K.-H. Lee, H. Sano, J. Han, T. Ichii, K. Murase and H. Sugimura, *Jpn. J. Appl. Phys.*, 2008, **47**, 307–312.

21. H. Sugimura, T. Shimizu and O. Takai, *J. Photopolym. Sci. Technol.*, 2000, **13**, 69–74.

22. Y. J. Kim, J. Han, H. Sano, K. H. Lee, K. Noda, T. Ichii, K. Murase, K. Matsushige and H. Sugimura, *Appl. Surf. Sci.*, 2009, **256**, 1507–1513.

23. T. Ye, E. a McArthur and E. Borguet, *J. Phys. Chem. B*, 2005, **109**, 9927–9938.

24. J. Yang, T. Ichii, K. Murase, H. Sugimura, T. Kondo and H. Masuda, *Chem. Lett.*, 2012, **41**, 392–393.

25. M. Rosso, M. Giesbers, K. Schröen and H. Zuilhof, *Langmuir*, 2010, **26**, 866–872.

26. L. Hong, K. Hayashi, H. Sugimura, O. Takai, N. Nakagiri and M. Okada, *Surf. Coatings Technol.*, 2003, **169-170**, 211–214.

27. N. A. Bullett, D. P. Bullett, F.-E. Truica-Marasescu, S. Lerouge, F. Mwale and M. R. Wertheimer, *Appl. Surf. Sci.*, 2004, **235**, 395–405.

28. A. Hennig, H. Borcherding, C. Jaeger, S. Hatami, C. Würth, A. Hoffmann, K. Hoffmann, T. Thiele, U. Schedler and U. Resch-Genger, *J. Am. Chem. Soc.*, 2012, **134**, 8268–8276.

29. V. I. Povstugar, S. S. Mikhailova and A. A. Shakov, *J. Anal. Chem.*, 2000, **55**, 405–416.

30. D. S. Everhart and C. N. Reilley, *Anal. Chem.*, 1981, **53**, 665–676.

31. S. Takabayashi, K. Okamoto, H. Motoyama, T. Nakatani, H. Sakaue and T. Takahagi, *Surf. Interface Anal.*, 2010, **42**, 77–87.

32. L. A. Langley, D. E. Villanueva and D. H. Fairbrother, *Chem. Mater.*, 2006, **18**, 169–178.

33. Y. Xing, N. Dementev and E. Borguet, *Curr. Opin. Solid State Mater. Sci.*, 2007, **11**, 86–91.

34. C. R. Hurley and G. J. Leggett, *ACS Appl. Mater. Interfaces*, 2009, **1**, 1688–1697.

35. N. Vandencasteele and F. Reniers, *J. Electron Spectros. Relat. Phenomena*, 2010, **178-179**, 394–408.

36. A. Ulman, *Chem. Rev.*, 1996, **96**, 1533–1554.

37. A. Hozumi, H. Taoda, T. Saito and N. Shirahata, *Surf. Interface Anal.*, 2008, **40**, 408–411.

38. A. Lehner, G. Steinhoff, M. S. Brandt, M. Eickhoff and M. Stutzmann, *J. Appl. Phys.*, 2003, **94**, 2289–2294.

39. R. S. Clegg and J. E. Hutchison, *Langmuir*, 1996, **12**, 5239–5243.

40. R. M. Silverstein, F. X. Webster and D. J. Kiemle, in *Spectrometric identification of organic compounds*, John Wiley & Sons Inc., Hoboken, NJ, USA, 7th Ed., 2006, pp. 120–124.

41. L. Sun, R. M. Crooks and A. J. Ricco, *Langmuir*, 1993, **9**, 1775–1780.

42. J. Kalia and R. T. Raines, *Angew Chem Int Ed*, 2008, **47**, 7523–7526.

43. D. D. M. Wayner and R. A. Wolkow, *J. Chem. Soc. Perkin Trans. 2*, 2002, **2**, 23–34.

Table of contents
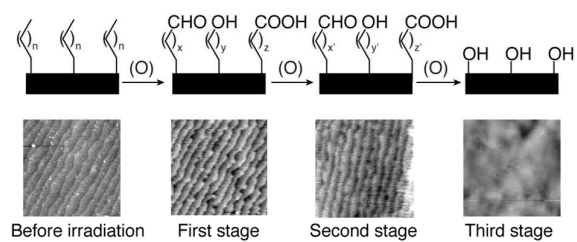
We followed the chemical constituents, surface properties, and morphology of the photo-modified alkyl self-assembled monolayers, which exposed to the active oxygen species generated from the vacuum ultraviolet irradiation.